JOURNAL OF MATERIALS SCIENCE LETTERS 24 (1989) 4120–4127

A novel method of introducing PbO dopant and (the study of) its influence on the electrical properties of semiconducting $Cd_{2-x}Pb_xSnO_4$ thick films

M. S. SETTY
Thick Film Materials, Physical Chemistry Division, National Chemical Laboratory, Poona 411 008, India

The sheet resistance of Cd_2SnO_4 thick films was reduced from 15 580 to 0.09 kΩ with respect to dopant concentration and peak firing temperature (600 to 900° C). Distinct colour changes were observed in these films. The inorganic binder introduced an impurity which greatly induce changes in its electrical properties. The Arrhenius relation ($\log R$–$10^3/T$) generally indicated slopes of 2 to 3 for all the compositions of $Cd_{2-x}Pb_xSnO_4$ (x = 0.002, 0.01, 0.02, 0.04 and 0.1). The donor ionization energies (E_d) varied from 0.01 to 0.76 eV. Resistance measurements during heating–cooling cycles indicated the possible presence of structural defects such as oxygen vacancies and cadmium interstitials. The oxidation of dopant ($Pb^{2+} \rightarrow Pb^{4+} + 2e'$) contributed in a major way to the overall conductivity. Scanning electron micrographs showed a progressive network formation due to sintering, thus contributing to the carrier mobility.

1. Introduction

Shannon *et al.* [1] reported two methods of introducing additional charge carriers to increase conductivity in Cd_2SnO_4: by creating oxygen vacancies and by chemical doping. The former process was reversible and the carriers thus created could be removed by heating in air/O_2 at 500 to 1000° C. The latter method was stable and was relatively unaffected by heating or by atmospheric exposure. Shannon *et al.* studied antimony-doped Cd_2SnO_4 ($Cd_2Sn_{1-x}Sb_xO_4$). The ϱ–T curve was characteristic of a metal or a semi-metal, whereas $CdIn_{2-x}Sn_xO_4$ had a lower conductivity than the corresponding oxygen deficient one.

Haacke *et al.* [2] reported the influence of additives on the properties of Cd_2SnO_4 thin films, mentioning that the inclusion of indium or lead tend to improve the clarity of the sputtered films.

Miyata *et al.* [3] also studied the effect of indium doping on electrical properties of Cd_2SnO_4 thin films. Haacke *et al.* [4] investigated the influence of doping elements in the sputtered Cd_2SnO_4 films. They reported an increase in carrier mobility with tantalum doping with respect to firing temperature ($Cd_2Sn_{0.98}Ta_{0.02}O_4$), and also found indium, antimony and tantalum to be donors when cadmium was substituted by indium and tin by antimony and tantalum. However, tantalum solubility was limited to 2 at % and the measured electron concentration before heat treatment was $1.7 \times 10^{20}\,cm^{-3}$.

Interest in the study and application of Cd_2SnO_4 thin films had been tremendous, but it has been scanty regarding the doping action on the electrical properties of Cd_2SnO_4 thick films.

In this paper a novel method of introducing PbO dopant into the matrix of the Cd_2SnO_4 host material is presented. We have tried, with the help of experimental data, to explain how the dopant in addition to the structural defects has increased the electrical conductivity.

2. Experimental procedure

The preparation details of the Cd_2SnO_4 paste formulations, thick film deposition and other processing parameters have already been reported [5].

It was observed that during the firing of these films in the thick-film furnace, they showed distinct colour and conductivity changes between those with and without glass for the same processing conditions. These significant observations led to the detailed investigation. At the outset, it was presumed that there could be two valence states of tin, i.e. Sn^{2+} and Sn^{4+}. The increase in conductivity was attributed to the hopping of electrons between the two tin sites. During the material preparation for Mössbauer studies, it was necessary to avoid glass because the films were very adherent to the substrate, but the changes observed were then absent in the glass-free samples. It was surmised therefore that the glass was responsible for altering the conditions. The individual component oxides of the glass corresponding to the weight taken, were mixed separately with Cd_2SnO_4 for paste formulations. The six oxides (PbO, SiO_2, Al_2O_3, B_2O_3, ZrO_2 and ZnO) were taken in five ratios and the films were fired at five different temperatures. Thus after screening nearly 150 samples, it was established that PbO was responsible for the colour change from yellow to green and for the conductivity increase.

0022–2461/89 $03.00 + .12

TABLE I Dopant concentration and compositions of the samples based on the glass percentages

Glass (%)	Pb (%)	Composition
0.1	0.066	$Cd_{1.988}Pb_{0.002}SnO_4$
0.5	0.33	$Cd_{1.99}Pb_{0.01}SnO_4$
1.0	0.66	$Cd_{1.98}Pb_{0.02}SnO_4$
2.0	1.32	$Cd_{1.96}Pb_{0.04}SnO_4$
5.0	3.33	$Cd_{1.9}Pb_{0.1}SnO_4$

The compositions calculated corresponding to different glass percentages, are shown in Table I.

X-ray analysis [5, 6] of the samples confirmed that PbO had been included in the Cd_2SnO_4 matrix. The unit cell volume increased with the peak firing temperature.

3. Measurements

3.1. Sheet resistivity

Nozik [7] carried out the conductivity measurements in the temperature range 77 to 300 K for thin films and bulk Cd_2SnO_4. Shannon *et al.* [1] presented the results of the variation of ϱ with T for single crystals up to 300 K. Miyata *et al.* [8] conducted measurements in the temperature range 100 to 295 K for thin films. In the present work, the measurements were carried out at 300 to 460 K.

For all thick film compositions, the firing conditions were fixed at 600, 700, 800 and 900° C for 20 min. Ohmic contacts (dI/dV = constant) were provided by applying air-drying silver paste. Other materials reported in the literature are indium [4], and vacuum-evaporated silver [9].

The teflon-mounted sample with press contacts was maintained at a set temperature in a tubular furnace. The thick films were annealed at 180° C for 2 h under vacuum.

The resistance measurements were made by calculating the circuit current passing through a standard resistor (connected in series) when a potential was applied across it. No polarity effect was observed.

It is seen from Table II that the resistance decreases with firing temperature for a given dopant concentration. A minimum value is obtained, for each FT 0.02 mol % PbO seems to be the optimum quantity to obtain very high conductivity. Representative Arrhenius plots for the films fired at 700 and 900° C are shown in Figs 1 and 2. Curves A to E represent the compositions $Cd_{2-x}Pb_xSnO_4$ where x = 0.002, 0.01, 0.02, 0.04 and 0.1. These curves have slopes of 2 or 3. The transition temperatures at which the low slope changes to a high slope are shown in the Table III for

TABLE II Sheet resistance (kΩ) dependence on PbO concentration and firing temperature (FT)

FT (° C)	Sample colour	Dopant concentration ($Cd_{2-x}Pb_xSnO_4$)				
		x = 0.002	0.01	0.02	0.04	0.10
600	Bright yellow	15850.00	588.00	60.30	234.50	505.80
700	Yellow ochre	118.00	48.80	18.90	10.70	33.80
800	Green	8.50	9.70	2.10	5.70	6.20
900	Green	0.50	0.52	0.09	0.22	0.64

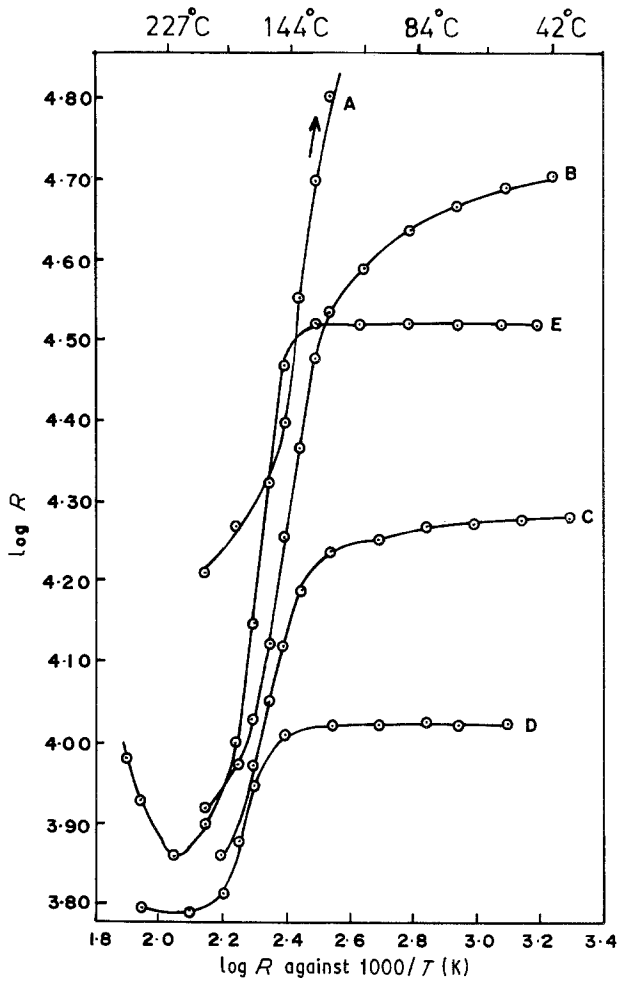

Figure 1 Samples fired at 700° C.

all the samples. The transition temperature is the lowest (84° C) at the lowest dopant concentration (for all FTs) and at lowest FT (for all dopant concentrations). As the dopant concentration increases, this also increases to 97, 127 and 144° C.

The activation energies were calculated from the Arrhenius plots. The ΔE values corresponding to the different slopes of the curves are tabulated in Table IV. The activation energy values are derived from the temperature ranges 300 to 384 K, 300 to 397 K and 300 to 427 K. The ΔE value decreases with FT, for all dopant concentrations. The trend is similar to the resistance changes with respect to firing temperature.

3.2. Current–voltage relation

A sudden drop in resistance of the samples at around 180° C was observed during conductivity measurements. It was thought to be due to filamentary action or to the creation of conductive paths. It was therefore worthwhile to see whether a similar change occurred under applied voltage.

TABLE III Transition temperatures (° C) at which the change of slopes takes place

FT (° C)	Dopant concentration ($Cd_{2-x}Pb_xSnO_4$)				
	x = 0.002	0.01	0.02	0.04	0.10
600	84	97	84	84	84
700	84	97	97	127	144
800	84	97	97	127	144
900	84	97	97	127	144

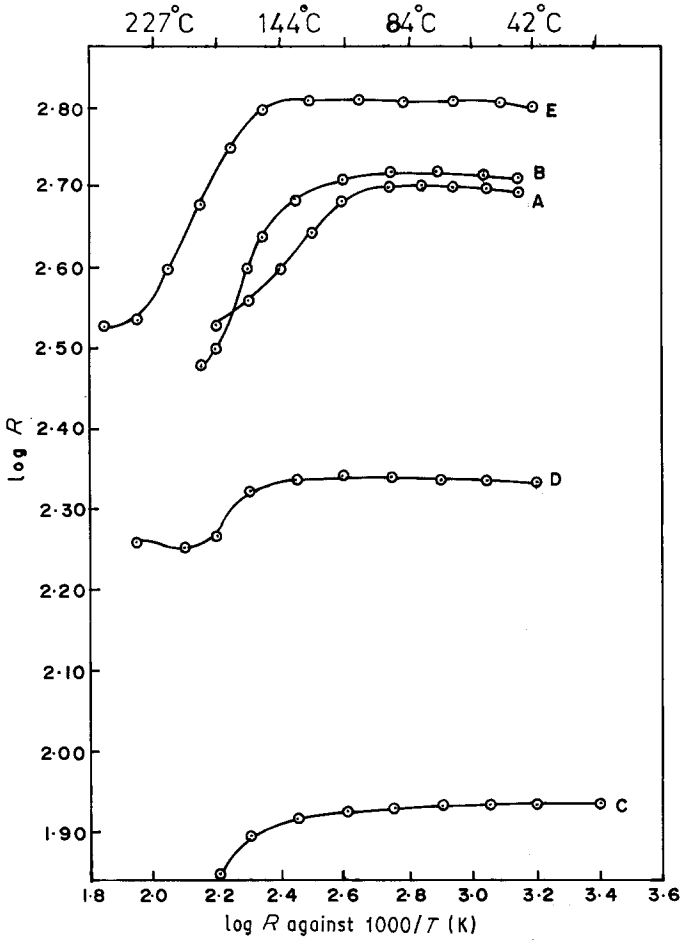

Figure 2 Samples fired at 900° C.

95 parts Cd_2SnO_4 and 5 parts glass frit were mixed under acetone, pelleted and fired at 700 to 900° C under identical conditions to the thick films.

After firing, a colourless glassy appearance was observed on the alumina substrate below the pellets, although the pellets showed a colour transformation.

3.2.1. Sample holder

The pellet is placed between the stationary and the spring-loaded movable brass discs which were electrically separated by a perspex block, Fig. 3. A d.c. regulated power supply (Aplab 0–60 V; 0–2.5 A, Model 7122) was used for applying the potential across the sample. The current was measured by a digital multimeter.

The current increased with the voltage, initially slowly and then fast, conforming to the non-linear relation with voltage. The I–V characteristics for all the samples are shown in Fig. 4.

The threshold voltage and the voltage gradient decreased with the sample firing temperature. Several cycles of I–V measurements are shown in Fig. 5 for the sample fired at 700° C. These show, on each successive cycle, a change in the current voltage relation. Thermal switching took place slightly at a lower V_{Th} than the previous value except in the case of the 900° C fired sample where it was constant, but the holding current increased with each cycle.

In one of the samples, arching occurred at a spot and it became scratch resistant. This was repeated at every cycle. Further, there was a time lag for the sample to return to the original state after withdrawing the applied voltage. It took 5 to 6 h for the 900° C fired sample and a long time (days) in the other two samples.

3.3. Seebeck coefficient

$Cd_{1.9}Pb_{0.1}SnO_4$ was selected as a typical composition for these measurements. Prints of 2 mm × 10 mm were deposited on 96% alumina substrates and fired at 600 to 900° C. Air-drying silver paste was applied to the film leaving an interelectrode distance of 6 mm. The thermo e.m.f. apparatus is shown in Fig. 6.

Two mica pieces were fixed on two teflon blocks with a 3 mm gap. The sample with a tin oxide-coated

TABLE IV Activation energies (eV) corresponding to the low (L) and high (H) slopes of log R–$10^3/T$ curves

FT (°C)	PbO (mol %)									
	0.002		0.01		0.02		0.04		0.1	
	L	H	L	H	L	H	L	H	L	H
600	0.12	0.76	< 0.01	0.33	0.04	0.24	0.03	0.12	< 0.01	0.20
700	0.04	0.65	0.02	0.44	< 0.01	0.27	< 0.01	0.22	< 0.01	0.72
800	0.03	0.46	< 0.01	0.16	< 0.01	0.16	< 0.01	0.20	< 0.01	0.18
900	< 0.01	0.08	< 0.01	0.06	< 0.01	0.06	< 0.01	0.09	< 0.01	0.14

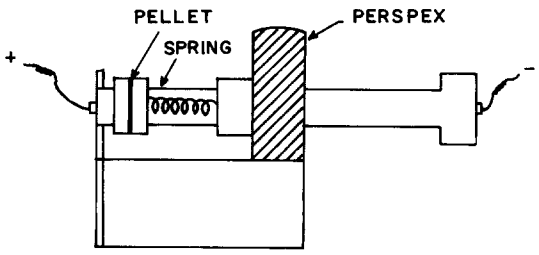

Figure 3 Sample holder for current–voltage measurements.

microheater under one of its ends was fastened by phosphor bronze clamps. Resin-enamelled copper wires were soldered to the clamps for power supply. Copper–constantan thermocouples were soldered on to the silver electrodes with the junction tips touching the sample ends. Shielded wires were used for external connections. The glass envelope was fitted into a copper case and the lead wires were taken through copper tubes. Proper earthing was provided to the whole system to avoid any electrostatic pick up.

The copper leads of the thermocuples measured the e.m.f. The apparatus was kept in a thermostat (VEB, Model U-10, DDR) which could maintain -60 to $+300°$ C with a regulating accuracy of $\pm 0.02°$ C. A Philips PW1500 DC micro voltmeter recorded the thermo e.m.f. and sample temperatures. The relation of thermo e.m.f. with sample temperature for the samples is presented in Fig. 7. It is seen from the figure that the Seebeck coefficient is negative for the samples fired at 600 to 900° C. It varies from -7 to $-127\,\mu V\,°C^{-1}$. θ is constant at $-7\,\mu V\,°C^{-1}$ for the 600° C fired sample and does not vary with sample temperature. However, it increases its negative value from -17 to $-23\,\mu V\,°C^{-1}$ for the 700° C sample; from -24 to $-33\,\mu V\,°C^{-1}$ for the 800° C sample and from -77 to $-127\,\mu V\,°C^{-1}$ for the 900° C sample. In the higher firing temperatures, θ increases with sample temperature, similar to a metal.

4. Sintering of the films

Sintering is an inherent property in thick films. The material is essentially polycrystalline and is constituted from very fine particles. During firing, the particles fuse to form clusters depending on the extent of firing conditions. The clusters thus formed are joined together to form a continuous network path. The barriers between the grain boundaries disappear. Morphological changes are shown in the scanning electron micrographs in Fig. 8.

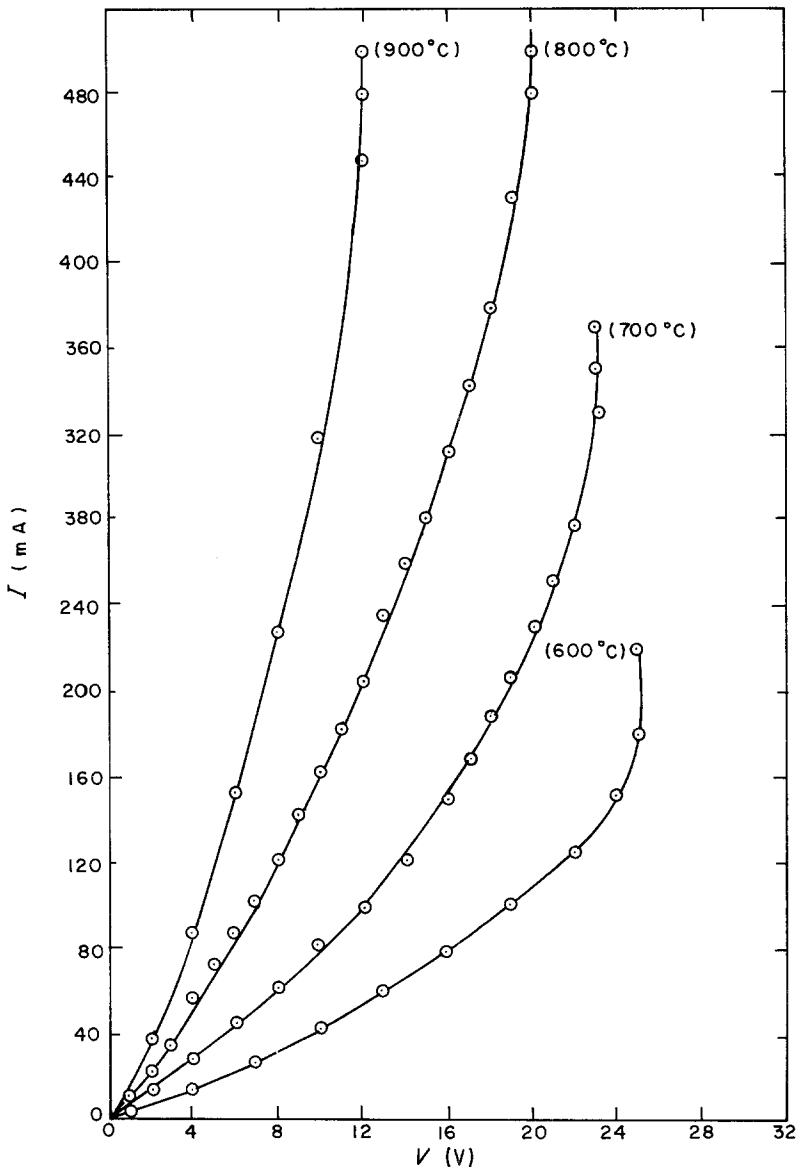

Figure 4 I–V characteristics of $(Cd_{1.9}Pb_{0.1}SnO_4)$ pellets fired at 600 to 900° C.

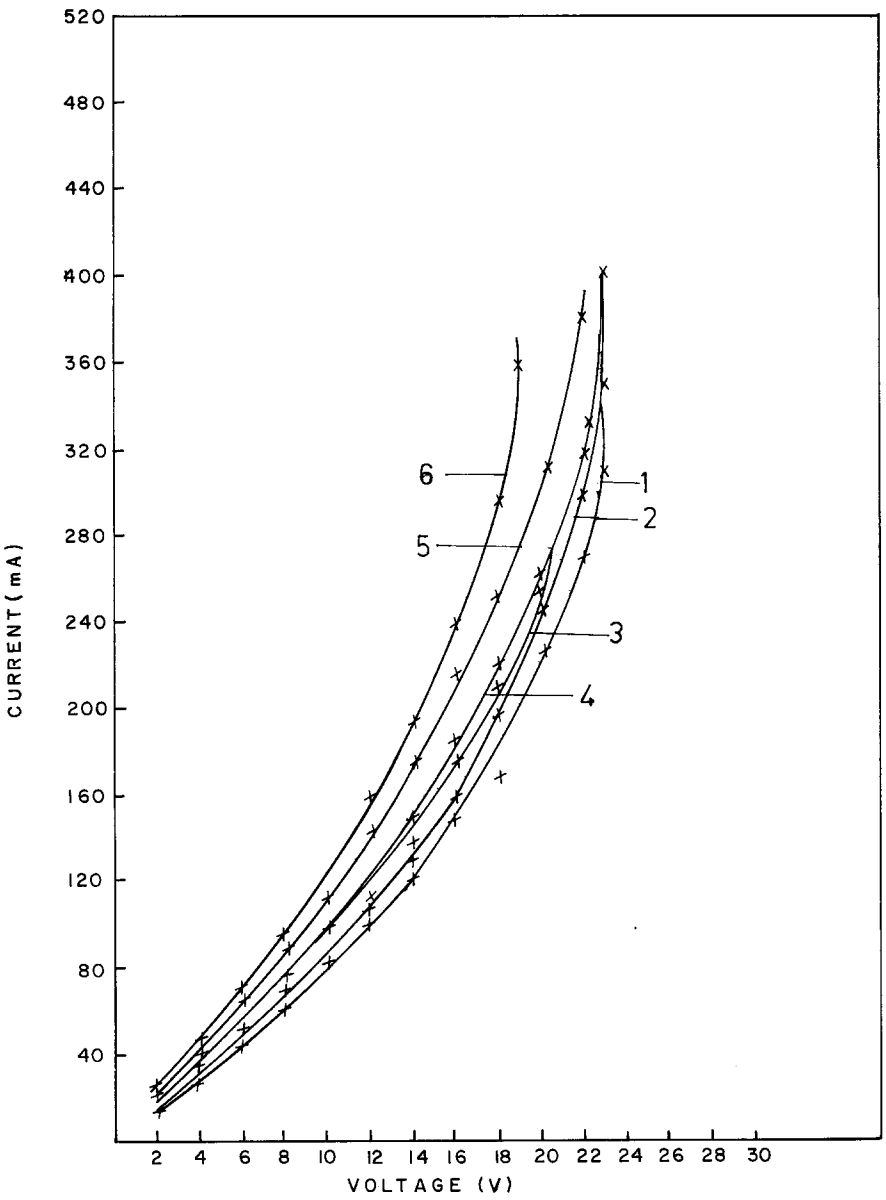

Figure 5 Current–voltage relation for 700° C fired sample.

5. Discussion

Electrical conductivity is given by $\sigma = ne\mu$ [10]. The carrier concentration increase is due to the structural defects such as anion vacancies or the cation interstitials and to the doping.

The doping action is considered first. Consider lead occupying a cadmium or tin site in the Cd_2SnO_4 matrix and its oxidation state. A list of possible substitutions and the oxidation states of lead is presented in Table V. The first three possibilities are ruled out because the samples have n-type conductivity. The fourth substitution is therefore applicable.

The resistance decreases (Table II) with the increase in dopant concentration, reaches a minimum value and then increases with further increase in its content. This trend is true for every firing temperature.

The lead is substitutionally incorporated at the cadmium site in the Cd_2SnO_4 matrix and its subsequent oxidation ($Pb^{2+} \rightarrow Pb^{4+} + 2e'$) is responsible for the large increase in conductivity. XPS spectra [6] show an increase in Pb^{4+}/Pb^{2+} ratio with respect to firing temperature. This goes on sponsoring electrons to the matrix and reaches a maximum. A donor band is formed because of several closely situated donor levels.

TABLE V

Substituting ion	Substituted ion	Resulting situation
Pb^{2+}	Cd^{2+}	No change
Pb^{2+}	Sn^{4+}	p-type
Pb^{4+}	Sn^{4+}	No change
Pb^{4+}	Cd^{2+}	n-type

However, this situation does not continue with further addition of Pb^{2+}. Once the lead ion occupies a tin site, its valence bonds are satisfied. The earlier hopping of electrons from Pb^{2+} to Pb^{4+} is reduced. Depending on the surroundings and Pb^{2+} concentration, a lead pair occurs (Pb^{2+}–Pb^{4+}). This couple formation eliminates some of the donor levels and does not contribute to the conductivity. Moreover, a possible occupation of Sn^{4+} by Pb^{2+}, which cannot be ruled out, will counter or nullify the contribution of electrons and thus decrease conductivity.

Similar results have been reported [11] in the case of tin-doped In_2O_3 films where a neutral complex (Sn^{2+}–Sn^{4+}) couple formation is mentioned.

The supporting experimental back up for the above reasoning can be seen from X-ray diffraction data [5]. It tells us that there is an increase in the unit cell

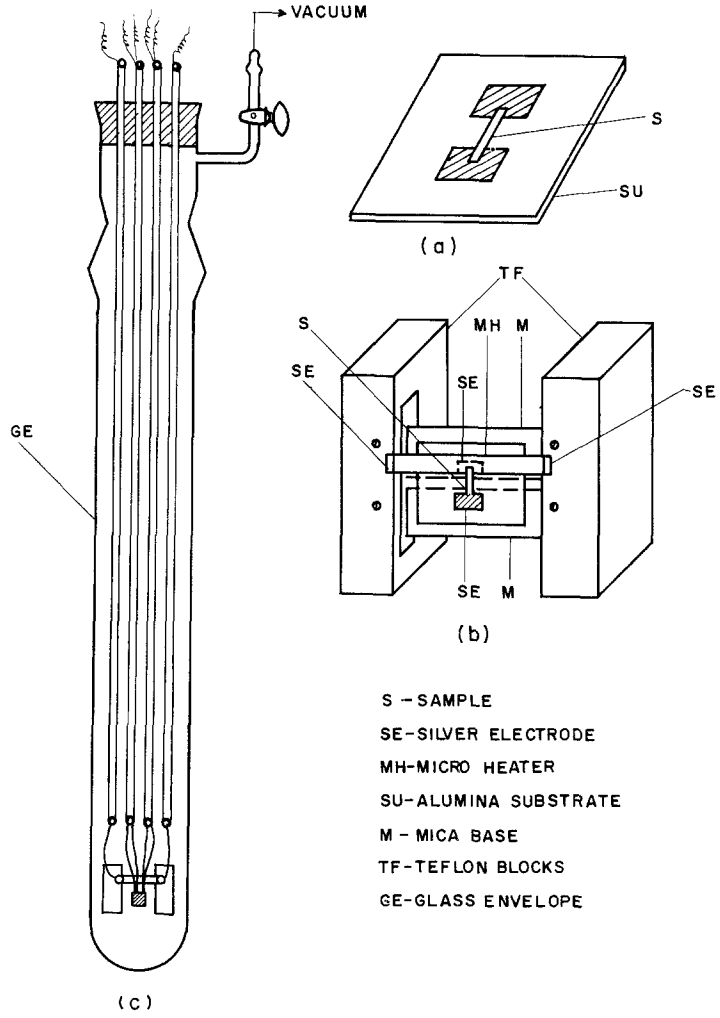

Figure 6 Sample holder for thermo e.m.f. measurement.

volume from sample to sample. This is governed by the presence of different ions in the Cd_2SnO_4 matrix and their occupation. The initial large increase of unit cell volume 0.0036 nm^3 from 600 to 700° C is attributed to the induction of Pb^{2+} (r = 0.121 nm) substituting Cd^{2+} (r = 0.097 nm). XPS data show that Pb^{4+} increases with FT. The ionic radius of Pb^{4+} is 0.084 nm (< Pb^{2+} or Cd^{2+}). This means that the increase in unit cell volume is smaller compared to the earlier value. So the formation of Pb^{4+} is confirmed by XPS and XRD results.

The activation energy data (Table IV) are consistent with the above argument. It is minimum at an optimum value of the dopant concentration, more so for 800 to and 900° C fired samples. This indicates the presence of many donor levels in the donor band. The increase in the donor ionization energy is attributed to the (Pb^{2+}–Pb^{4+}) couple formation which has eliminated the corresponding energy levels. Higher energy is therefore required to excite the electrons from the donor band to the conduction band.

The as-fired sample always possessed a high resist-

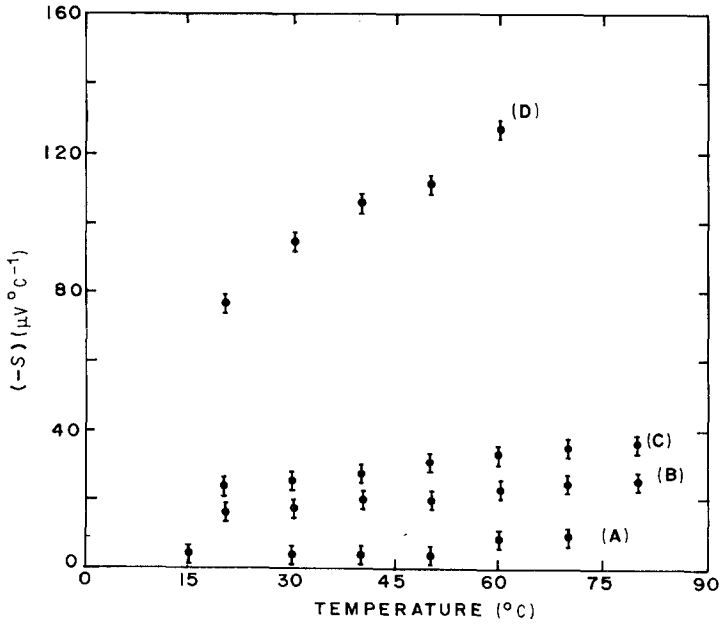

Figure 7 Variation of Seebeck coefficient (S) with temperature for ($Cd_{1.9}Pb_{0.1}SnO_4$) thick films fired at (A) 600° C, (B) 700° C, (C) 800° C and (D) 900° C.

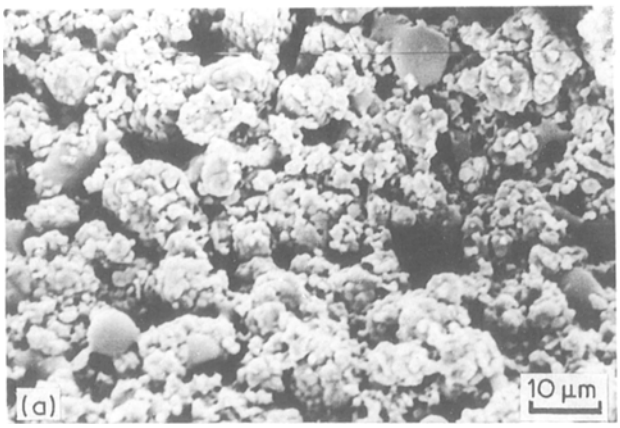

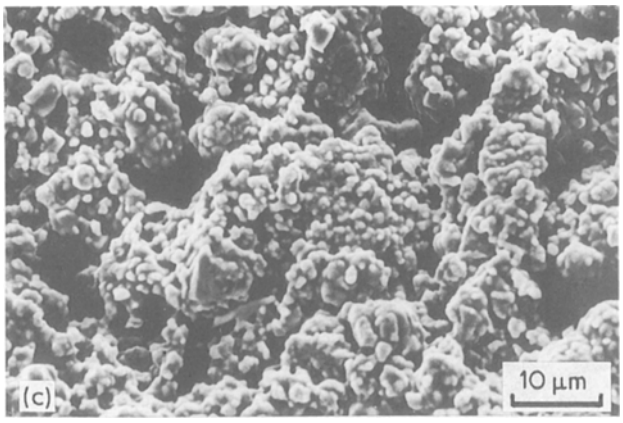

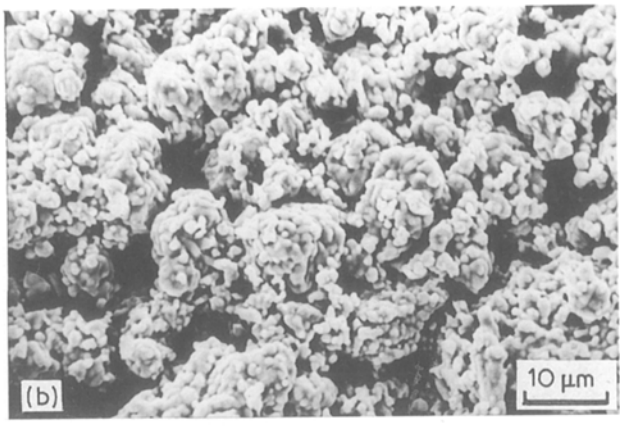

Figure 8 Scanning electron micrographs of $Cd_{1.9}Pb_{0.1}SnO_4$ fired thick films. (a) 500° C, (b) 700° C and (c) 900° C.

ance value, notwithstanding the dopant concentration and other preparation parameters. The value decreased by 1 to 2 orders of magnitude after annealing at 180° C under vacuum. Heat treatment of Cd_2SnO_4 thin films under vacuum and in the reforming atmosphere also showed a conductivity increase and was found to be highly temperature dependent [12].

A wide variation in resistance is reported [13] even in the sputtered films, both doped and undoped. This seems to be a common phenomenon with all the oxygen-deficient semiconductors (In_2O_3, SnO_2, CdO, etc.). Thornton and Hedgcoth [9] suggested liberation of carriers from the compensation traps during heat treatment.

Several controlling factors therefore influence the electrical properties, such as oxygen vacancies, cation interstitials, dissociation of oxides, adsorption–desorption of oxygen, diffusion of defects, sintering of particles, etc.

Evaporating of cadmium as CdO is negligible in the temperature range 1150 to 1374 K [14, 15]. However, dissociation of CdO is possible. The defect comprises "D" centres [16]. The binding energy of the second electron in the "D" centre is low and acts as an effective electron donor. If the donor states provided by oxygen vacancies are considered to be doubly ionized, then the ionization energy is less. This explains our low values of activation energy.

The following structural defects are considered which enhance the conductivity.

5.1. Oxygen vacancies

Chol *et al.* [17] proposed the transport mechanism involving oxygen vacancies in the anion sublattice of CdO. They carried out conductivity measurements under different partial pressures of oxygen. They stated:

$$O_0 = V_0 + 2e' + 1/2\ O_2(g) \quad (1)$$

Many other workers [7, 13, 18, 19] reported the presence of oxygen vacancies in Cd_2SnO_4. The defects produce donor states in the forbidden gap.

In our earlier studies [5], XPS spectra indicated two oxygen peaks corresponding to the bound and chemisorbed oxygen. The desorption of oxygen contributed to the conductivity. The as-fired samples which were highly resistive but decreased on annealing under vacuum, switched back to the original state when heat treated in air. The thermal analysis studies indicated a gain in weight when Cd_2SnO_4 was heated in air.

It was observed that diffusion of oxygen takes place from within the film to the surface. The Seebeck coefficient increased with time, denoting the increase of electrons because of this diffusion.

Resistance measurements during heating–cooling (H–C) cycles disclosed the time-dependent nature for the $Cd_{1.9}Pb_{0.1}SnO_4$ thick films.

The current–voltage results showed the temperature increase when voltage was applied. This was due to Joule heating. Heat dissipation depended on the several factors such as compaction, particle size, etc. During this heating, the adsorbed oxygen was ionized and released to the surface leaving behind two conduction electrons per atom [9]. The diffused oxygen in the bulk also migrates to the surface and is desorbed. This transportation contributes to the conductivity. The increase in current at a particular voltage was time dependent, indicating that the oxygen in the bulk requires time to diffuse out. The conductivity during H–C cycles, and the Seebeck coefficient increase with time and other data also led to the same result, i.e. desorption of oxygen contributing to conductivity.

5.2. Cadmium interstitials

$$Cd_i^{\times} \rightarrow Cd_i + e' \quad (2)$$

Ionized cation interstitials are formed. This means transferring of a neutral cadmium atom from the vapour phase to an interstitial position. According to Koffyberg [20] Cd_i was completely ionized in CdO.

$$Cd_i = Cd_i + e' \quad (3)$$

$$Cd_i^x = Cd_i + 2e' \quad (4)$$

The equilibrium condition where doubly ionized Cd_{Cd} existed in the Cd_2SnO_4 matrix could be written as follows

$$Cd_{Cd} + O_0 \rightarrow Cd_i + 2e' + 1/2\ O_2(g) \quad (5)$$

Thermal analysis results [5] showed a weight loss during Cd_2SnO_4 formation. Thermo e.m.f. data (linear dependence of Seebeck coefficient with temperature) have shown that Cd_2SnO_4 was not stoichiometric. Cd_2SnO_{4-x} or free cadmium might be present as an outside phase. XPS [5] exhibited a gradual increase of cadmium phase on the surface with FT. There was an increase in the ratio of peak heights (intensities) of $Cd3D_{5/2}$ and $Sn3d_{5/2}$ core electron spectra.

Hall [21] was also of the opinion that cadmium interstitials and oxygen vacancies provided the conduction electrons in the sputtered Cd_2SnO_4 films. In In_2O_3, the conduction was reported to be due to indium interstitials.

Very high conductivity values were obtained for all the compositions fired at 900° C. Here the clusters of loosely bound particles coalesced and sintered, thus reducing the number of barriers at the grain boundaries. This increased the carrier mobility because of the increase in contact area [14]. It is well-known that carrier mobility decreases with the increase in current carriers because of scattering. This situation is different in the present case. Most of the carrier concentration increase is up to 700° C. The carrier mobility increases from this stage. The scanning electron micrographs, Fig. 8, show a distinct cluster and network formation from 500 to 900° C fired samples. The void spaces are much smaller by comparison than the connecting necks and these are shorter (Fig. 8c).

6. Conclusions

The electrical conductivity data show the major contribution coming from the PbO dopant. Other experimental results such as XPS, XRD, *I–V* characteristics, thermal analysis and thermo e.m.f. revealed the presence of oxygen vacancies and cadmium interstitials. The carrier mobility is inferred from the diffuse reflectance [22] and sintering effect results, though for different reasons: one is due to the low effective electron mass and the other to the annihilation of grain-boundary barriers. Thus we see that the increase in conductivity is due both to the increase in carrier concentration and carrier mobility. This looks strange, because it contradicts the semiconductor theory, but it is true. The carrier concentration increases up to 700° C and from there on carrier mobility contributes to the increase in conductivity.

References

1. R. D. SHANNON, J. L. GILSON and R. J. BOUCHARD, *J. Phys. Chem. Solids* **38** (1977) 877.
2. G. HAACKE, H. ANDO and W. E. MEALMAKER, *J. Electrochem. Soc.* **124** (1977) 1923.
3. N. MIYATA, K. MIYAKE, H. NAKAOKA and YAMAGUCHI DIGAKU, *Koghakuka, Kenkyu Hokoku* **28** (1978) 235.
4. G. HAACKE, W. E. MEALMAKER and L. A. SIEGEL, *Thin Solid Films* **55** (1978) 67.
5. M. S. SETTY and A. P. B. SINHA, *ibid.* **144** (1986) 7.
6. M. S. SETTY, PhD thesis, Poana University (1983).
7. A. J. NOZIK, *Phys. Rev.* **B6** (1972) 453.
8. N. MIYATA, K. MIYAKE, T. FUKUSHIMA and K. KOGA, *Appl. Phys. Lett.* **35** (1979) 542.
9. J. A. THORNTON and V. L. HEDGCOTH, *J. Vac. Sci. Technol.* **13** (1976) 117.
10. N. B. HANNAY, "Solid State Chemistry" (Prentice-Hall International, Englewood Cliffs, New Jersey, 1967) p. 24.
11. H. KOSTIN, R. JOST and W. LEMS, *Phys. Status Solidi (a)* **29** (1975) 87.
12. P. LLOYD, Brit. Pat. 1519733 (1978); *Chem. Abstr.* 90:16154B.
13. G. HAACKE, *Ann. Rev. Mater. Sci.* **7** (1977) 73.
14. J. CHOISNET, A. DESCHANVRES and B. RAVEAU, *Compt. Rend.* **266c** (1968) 543.
15. E. F. LAMB and F. C. TOMPKINS, *Trans. Farad. Soc.* **68** (1964) 1424.
16. F. P. KOFFYBERG, *Solid State Commun.* **9** (1971) 2197.
17. JAC SHI CHOL, YOUNG HWAN KANG and KAU HONG KIM, *J. Phys. Chem.* **81** (1977) 2208.
18. M. TROMEL, *Naturwissen Schaften* **54** (1967) 17; *Chem. Abstr.* 67: 15815B.
19. S. MIYAKE, *Jpn Kokai, Tokyo Koho* **81** (1981) 134, 730; *Chem. Abstr.* 96: 61269 Y.
20. F. P. KOFFYBERG, *Can. J. Phys.* **49** (1971) 435.
21. DALE HALL, *J. Electrochem. Soc.* **124** (1977) 804.
22. M. S. SETTY, *J. Mater. Sci. Lett.* **6** (1987) 909.

Received 8 April 1988
and accepted 14 February 1989